

A Werner-Type Alkyl Cobalt(III) Compound: Formation of a Carbon–Cobalt Bond Demonstrated by ^{13}C , ^{59}Co NMR and X-Ray Structure Determinations

Pauli Kofod,^a Erik Larsen,^{a,*} Sine Larsen,^b Carsten H. Petersen,^a Johan Springborg^a and Dong-Ni Wang^a

^aChemistry Department, The Royal Veterinary and Agricultural University, Thorvaldsensvej 40, DK-1871 Frederiksberg and

^bDepartment of Chemistry, University of Copenhagen, Universitetsparken 5, DK-2100 Copenhagen, Denmark

Kofod, P., Larsen, E., Larsen, S., Petersen, C. H., Springborg, J. and Wang, D., 1992. A Werner-Type Alkyl Cobalt(III) Compound: Formation of a Carbon–Cobalt Bond Demonstrated by ^{13}C , ^{59}Co NMR and X-Ray Structure Determinations. – Acta Chem. Scand. 46: 841–853.

The coordinated alkyl cation (1,6-diamino-3-thia-4-hexanido)(1,4,7-triazacyclononane)cobalt(III), $[\text{Co}(\text{tacn})(\text{C-aeaps})]^{2+}$ has been prepared in aqueous solution by base addition to (3-thia-1,6-hexanediamine)(1,4,7-triazacyclononane)cobalt(III), $[\text{Co}(\text{tacn})(\text{aeaps})]^{3+}$. The unusual alkyl cobalt(III) coordination compound has been characterized by UV–VIS and NMR spectroscopy as well as X-ray crystallography. The ligand field band in the visible region is of the usual low intensity, and so the carbanion is an innocent ligand. Its Δ_{Oh} value seems not very different from that of an amine ligand. The coupling constants between the ^{59}Co and ^{13}C nuclei were determined for $[\text{Co}(\text{tacn})(\text{C-aeaps})]^{2+}$ and a few others to make comparisons possible. Single bonds are found to have $J_{\text{C-Co}}$ values of 80–90 Hz.

The starting material can be considered a Brønsted acid with the conjugate base being a carbanion complex. The starting material and its conjugate base were isolated as perchlorates, and they have been characterized by X-ray diffraction methods at 110 K. Both form orthorhombic crystals with space group *Pbca*. Crystal data for $[\text{Co}(\text{tacn})(\text{aeaps})](\text{ClO}_4)_3$: $M = 620.74 \text{ g mol}^{-1}$, $a = 28.094(4)$, $b = 10.580(3)$, $c = 14.620(1) \text{ \AA}$, $V = 4345(2) \text{ \AA}^3$, $F(000) = 2560$, $Z = 8$, $D_m = 1.882$, $D_{\text{calc}} = 1.898 \text{ g cm}^{-3}$, $\text{MoK}\alpha = 0.71073 \text{ \AA}$, $\mu = 13.21 \text{ cm}^{-1}$, $R = 0.042$ for 3590 unique reflections. Crystal data for $[\text{Co}(\text{tacn})(\text{C-aeaps})](\text{ClO}_4)_2$: $M_r = 521.29$, $a = 18.169(5)$, $b = 15.824(4)$, $c = 13.888(4) \text{ \AA}$, $V = 3993(3) \text{ \AA}^3$, $F(000) = 2168$, $Z = 8$, $D_{\text{calc}} = 1.734 \text{ g cm}^{-3}$, $\mu = 12.76 \text{ cm}^{-1}$, $R = 0.074$ for 1400 unique reflections. The latter compound displays disorder of both the cation and one of the perchlorate ions. The disorder of the $[\text{Co}(\text{tacn})(\text{C-aeaps})]^{2+}$ ion corresponds to the presence of the two different configurations of the carbon-bound ligand at the cobalt site.

Recently, two communications were published on the facile formation of Werner-type alkyl cobalt(III) coordination compounds.^{1,2} In one case the starting material was a cobalt(II) coordination compound as described in Scheme 1. The reaction seems complicated because of the necessity for the simultaneous presence of a strong ligand L (e.g. CN^-) and an oxidant.¹ The reaction was characterized as an oxidative dehydrogenation.¹ We found the other case (Scheme 2) to be a simple acid–base reaction which, however, is complicated by the possibility of a large number of isomers.²

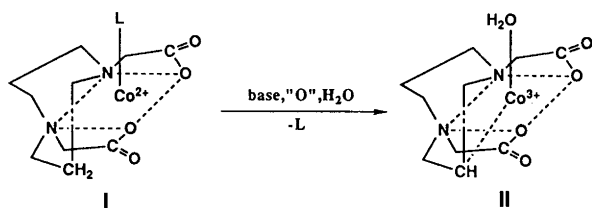
Both reactions were substantiated by the determination of the crystal structures by X-ray diffraction methods. The formation of cobalt(III)–carbon bonds is therefore established beyond doubt. Considering that previously studied formations of Co–C bonds were carried out under drastic conditions and that the products possess low stability, the abovementioned reactions seem worthy of further study.

* To whom correspondence should be addressed.

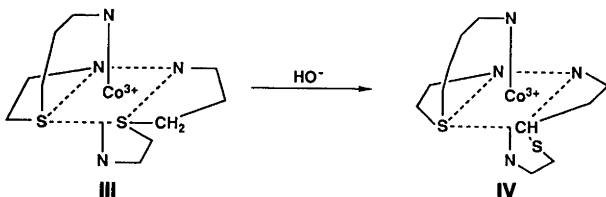
We have concentrated on a reaction similar to Scheme 2, but have simplified the problem by blocking one octahedral face with 1,4,7-triazacyclononane (tacn) while still using (2-aminoethyl)(3-aminopropyl)sulfide (aeaps) as the coordinated alkane acid. The reaction studied is shown in Scheme 3.

This paper includes details of the crystal structure determinations of a starting product $[\text{Co}(\text{tacn})(\text{aeaps})](\text{ClO}_4)_3$ and a reaction product $[\text{Co}(\text{tacn})(\text{C-aeaps})](\text{ClO}_4)_2$, where the anion of aeaps, 1,6-diamino-3-thia-4-hexanide, binds to cobalt at the 1-, 4- and 6-positions.

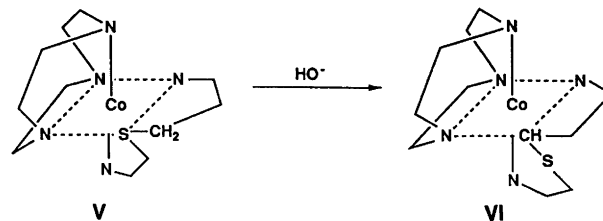
The base strength of a carbanion is so large that it is feasible that in aqueous solution VI has hydrolysed to VII. The structure of the product cation in aqueous solution was therefore studied by ^{13}C and ^{59}Co NMR in order to prove the existence of the Co–C bond in aqueous solution also. This is most convincingly done by measurements of the coupling constant. From lineshape analysis using both ^{13}C and ^{59}Co NMR resonances we have obtained the nuclear ^{13}C – ^{59}Co coupling constant, and it has been compared with



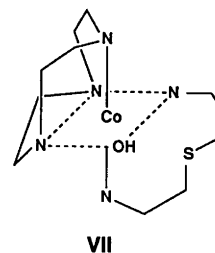
Scheme 1.



Scheme 2.



Scheme 3.



Scheme 4.

a few other systems. It appears that formerly only those C–Co coupling constants have been recorded that can be seen directly from splittings of ^{13}C NMR lines. This situation is met only in cubic symmetry, where the electric field gradient is zero. To our knowledge coupling constants have not formerly been reported in the literature for the biological relevant alkyl cobalt(III) coordination compounds.

Experimental

Preparations.

$[\text{Co}(\text{tacn})\text{Cl}_3]$. The neutral complex was prepared as described in the literature³ using $\text{tacn} \cdot 3\text{HCl}$ obtained as published by Searle and Geue.⁴

The thioether compounds $[\text{Co}(\text{tacn})(\text{daes})\text{Cl}_3]$ (daes = di(2-aminoethyl)sulfide) and $[\text{Co}(\text{tacn})(\text{aeaps})\text{Cl}_3]$ were prepared from $[\text{Co}(\text{tacn})\text{Cl}_3]$ and the free thioamines daes⁵ or aeaps⁶ in warm dimethylsulfoxide (DMSO):

$[\text{Co}(\text{tacn})(\text{aeaps})\text{Cl}_3 \cdot \text{H}_2\text{O}]$. A stirred suspension of 4.0 g (13.58 mmol) $[\text{Co}(\text{tacn})\text{Cl}_3]$ in 20 ml DMSO was heated to 85°C. 2 ml (15 mmol) aeaps were then added, upon which the colour changed from blue–green to brown. After 5 min there was still some unreacted $[\text{Co}(\text{tacn})\text{Cl}_3]$ left, so another 1 ml of aeaps was added. The suspension was stirred for 15 min at 85°C and then allowed to cool to room temperature. The brownish crystals were isolated by filtration, and washed with 3 ml DMSO and 3 × 15 ml ether–ethanol (1:1), giving 5.14 g (11.5 mmol) light brown $[\text{Co}(\text{tacn})(\text{aeaps})\text{Cl}_3]$. The product was recrystallized by dissolving 4.64 g $[\text{Co}(\text{tacn})(\text{aeaps})\text{Cl}_3]$ in 15 ml of water (70°C), leaving some unreacted $[\text{Co}(\text{tacn})\text{Cl}_3]$ to be filtered off. The red solution was evaporated under reduced pressure until precipitation commenced, and the crystallization was completed by adding ca. 50 ml of ethanol and cooling on ice. Filtration and washing with ethanol gave 4.15 g (9.29 mmol) orange $[\text{Co}(\text{tacn})(\text{aeaps})\text{Cl}_3 \cdot \text{H}_2\text{O}]$ (yield 68 %

from $[\text{Co}(\text{tacn})\text{Cl}_3]$). Analytical data: Calculated for $\text{C}_{11}\text{H}_{31}\text{N}_5\text{OSCl}_3\text{Co}$: C, 29.57; H, 6.99; N, 15.68; Cl, 23.81; Co, 13.19. Found: C, 29.32; H, 7.15; N, 15.69; Cl, 23.90; Co, 13.16.

The perchlorate is less soluble than the chloride salt and it was isolated from a solution of the chloride by the addition of a saturated solution of sodium perchlorate.

Electrochemical data for $[\text{Co}(\text{tacn})(\text{aeaps})\text{Cl}_3 \cdot \text{H}_2\text{O}]$ in 0.1 M aq. K_2SO_4 : $E^{\circ'} = -0.11$ V (vs. NHE).

$[\text{Co}(\text{tacn})(\text{daes})\text{Cl}_3 \cdot \text{H}_2\text{O}]$ was prepared by a procedure similar to that above. Reddish-orange crystals were obtained in high yield (83 %). Analytical data: Calculated for $\text{C}_{10}\text{H}_{29}\text{N}_5\text{OSCl}_3\text{Co}$: C, 27.76; H, 6.75; N, 16.18; S, 7.41; Cl, 24.58. Found: C, 27.75; H, 6.87; N, 15.77; S, 7.55; Cl, 24.28. $E^{\circ'} = -0.18$ V (vs. NHE).

$[\text{Co}(\text{tacn})(\text{C-aeaps})](\text{ClO}_4)_2$. A solution of $[\text{Co}(\text{tacn})(\text{aeaps})\text{Cl}_3 \cdot \text{H}_2\text{O}]$ (0.5 g, 1.1 mmol) in 1 M NaOH (10 ml, 10 mmol) was kept at 40°C for 90 min. During this time the colour changed from reddish-purple to brown. The solution was cooled in ice and 3 ml of a saturated solution of sodium perchlorate in water (room temperature) were added. Yellow–brown crystals of $[\text{Co}(\text{tacn})(\text{C-aeaps})](\text{ClO}_4)_2$ separated. After some minutes the crystals were filtered off and washed with 50 % ethanol, then 96 % ethanol and finally diethylether, and then dried in the air. Yield 0.48 g (90 %). This product only showed one component in its IE HPLC, and was considered pure. Analytical data: Calculated for $\text{C}_{11}\text{H}_{28}\text{N}_5\text{O}_8\text{SCl}_2\text{Co}$: C, 25.39; H, 5.42; N, 13.46; S, 6.16; Cl, 13.63; Co, 11.33. Found: C, 25.45; H, 5.30; N, 13.45; S, 6.30; Cl, 13.55; Co, 11.37. Electrochemical data for the coordination compound in acetonitrile (0.1 M $\text{N}(\text{Bu})_4\text{PF}_6$): $E^{\circ'} = -1.28$ V (vs. NHE).

Spectral measurements.

UV–VIS. A Perkin-Elmer diode array spectrophotometer was used for UV–VIS spectral measurements. Ion-exchange high-performance liquid chromatography was

Table 1. Thermodynamic parameters for deprotonation of $[\text{Co}(\text{tacn})(\text{aeaps})]^{3+}$ in 1 M $\text{Na}(\text{OH}, \text{ClO}_4)$ determined spectrophotometrically, eqns. (1) and (2).

$T/^\circ\text{C}$	$K_b(\text{obs})/1 \text{ M}$	$K_b(\text{calc})^a/1 \text{ M}$
0	0.309	0.296
25	0.420	0.433
40	0.900	0.898

^aThe values of $K_b(\text{calc})$ have been obtained by non-linear regression analysis, which gave the thermodynamic parameters in Table 2.

performed using a Waters HPLC system connected to a diode array detector. A Waters Protein Pak SP-5PW cation exchanger was used with 0.23 M Na_2SO_4 as eluent in all experiments, and the flow was normally 1.0 ml min^{-1} . All HPLC experiments were made at 25°C .⁷

NMR spectra were measured at 5.87 T on a Bruker AC 250 NMR spectrometer equipped with a 5 mm probe for ^{13}C NMR measurements or a 10 mm broad-band tunable probe for ^{59}Co NMR measurements. Deuterated solvents were used to provide a deuterium lock. Quadrature detection and quadrature phase cycling were always used.

^{13}C NMR spectra were obtained on a 14286 Hz spectral window with a digital resolution of 0.872 Hz per point. ^{13}C DEPT NMR spectra⁸ were used to achieve differentiation of the CH , CH_2 and CH_3 groups.

The type of compound investigated here has coupling constants J_{CH} of about 135 Hz, and therefore a delay time $\tau = 3.7 \text{ ms}$ was used. The ^{13}C DEPT NMR spectra shown in this paper were all obtained using $\theta = 3\pi/4$, and the phase of the spectra was corrected to make ^{13}C NMR signals from CH and CH_3 groups positive and those from CH_2 groups negative.

An additional line-broadening of 1 Hz was employed to the ^{13}C NMR spectra before Fourier transformation to improve the signal-to-noise ratio.

^{13}C chemical shift values (δ) are reported in ppm relative to internal 2,2-dimethyl-2-silapentane-5-sulfonate (DSS; $\delta = 0, 17.66, 21.74$ and 57.02 ppm) for D_2O solutions, or tetramethylsilane (TMS; $\delta = 0 \text{ ppm}$) for DMSO-d_6 and acetonitrile- d_3 solutions.

^{59}Co NMR spectra were obtained on a 166 667 Hz spectral window with a digital resolution of 10.2 Hz per point. ^{59}Co NMR signals with lines wider than about 5 kHz were measured using the RIDE (ring-down elimination) pulse sequence⁹ to suppress probe ringing. With this pulse sequence the dead-time could be reduced to 15 μs .

A 10–20 Hz additional line-broadening was employed to the ^{59}Co NMR spectra prior to Fourier transformation.

^{59}Co chemical shift values (δ) are reported in ppm relative to an external aqueous solution of $\text{K}_3[\text{Co}(\text{CN})_6]$ ($\delta = 0 \text{ ppm}$), using replacement of the sample.

Chemicals for NMR. Deuterium oxide, 99.8 atom % D; acetonitrile- d_3 , 99.5 atom % D were all from Sigma;

dimethylsulfoxide- d_6 , 99.8 atom % D, was from ICN Biochemicals.

Electrochemical measurements. Cyclic voltammetry was performed in a three-electrode cell using a gold as the working electrode and calomel as the reference electrode for aqueous solutions. The potential was controlled by a PAR 174A potentiostat, and the voltammograms were recorded on a Watanabe XY-plotter. Measurements on acetonitrile solutions were obtained with a mercury working electrode, a silver wire as a reference electrode and a Pt auxiliary electrode. The potentials were measured relative to anthracene. The formal reduction potentials obtained are reported relative to NHE (the normal hydrogen electrode).

Determination of base dissociation constants of coordinated amines. The equilibrium constant for the reaction of $[\text{Co}(\text{tacn})(\text{aeaps})]^{3+}$ in basic solution was determined spectrophotometrically. The spectra had to be measured as fast as possible, since the cobalt(III) complex in basic solution undergoes a relatively fast reaction to form the cobalt(III)-alkyl complex. Solutions of $[\text{Co}(\text{tacn})(\text{aeaps})]\text{Cl}_3 \cdot \text{H}_2\text{O}$ in 1 M NaClO_4 were mixed rapidly with an equal volume of 1 M $\text{Na}(\text{ClO}_4, \text{OH})$ using a flow cell, and the first spectrum was measured within 20–30 s. Additional spectra were recorded within the following 2 min, and the spectra at the time of mixing were calculated by linear extrapolations. These extrapolations were less than 2% from the first measured spectral data. In all experiments the concentration of $\text{Co}(\text{III})$ was about 10^{-3} M . The change of the molar absorption coefficient as a function of $[\text{HO}^-]$ followed the

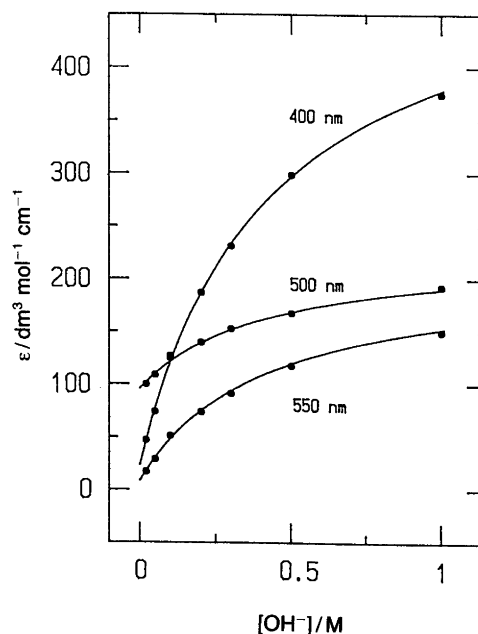


Fig. 1. Examples of changes of the molar absorption of a solution of $[\text{Co}(\text{tacn})(\text{aeaps})]\text{Cl}_3 \cdot \text{H}_2\text{O}$ as a function of $[\text{HO}^-]$ at 25°C and $l = 1.0 \text{ M}$. The solid lines represent calculated values.

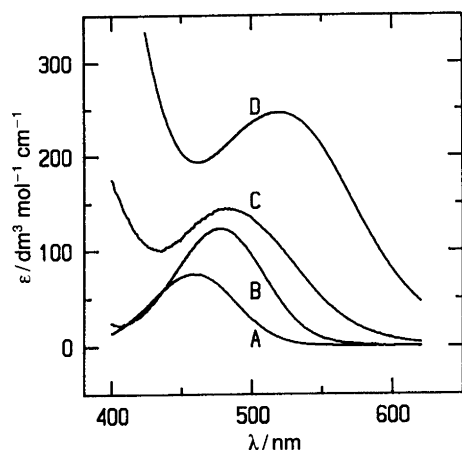


Fig. 2. The visible absorption spectra of $[\text{Co}(\text{tacn})(\text{aeaps})]^{3+}$ (B) and its base form (D) and of $[\text{Co}(\text{tacn})_2]^{3+}$ (A) and its base form (C) at $I = 1.0 \text{ M}$ (25°C).

expression shown in eqn. (1), which has been derived assuming that one single acid–base reaction occurs. In eqn. (1) ϵ_{HA} and ϵ_{A} are the molar absorption coefficients of

$$\epsilon(\text{obs}) = \frac{\epsilon_{\text{HA}} K_{\text{b}} + \epsilon_{\text{A}}[\text{HO}^-]}{K_{\text{b}} + [\text{HO}^-]} \quad (1)$$

the acid and basic forms of the cobalt(III) complex and $\epsilon(\text{obs})$ is the observed molar absorption coefficient. The values of ϵ_{HA} are known, and values of ϵ_{A} and K_{b} were then obtained by non-linear regression analysis using $\epsilon(\text{obs})$ -values measured at $\lambda = 400, 450$ and 550 nm (Table 1 and Fig. 1). From the value of K_{b} and the spectra in 1 M NaClO_4 and in 1 M NaOH the spectrum of the basic form, $[\text{Co}(\text{tacn})(\text{aeaps-N}^-)]^{2+}$, was then calculated (Figs. 2 and 3). Measurements using $5 \text{ M Na}(\text{NO}_3, \text{OH})$ gave a similar result (Table 2). The base dissociation constants of $[\text{Co}(\text{tacn})_2]^{3+}$ and $[\text{Co}(\text{tacn})(\text{daes})]^{3+}$ were determined in the same way using $1 \text{ M Na}(\text{ClO}_4, \text{OH})$ at 25°C (Table 2).

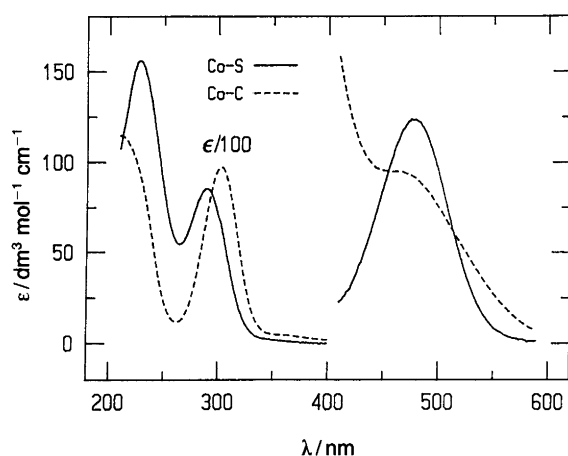


Fig. 3. The molar visible and ultraviolet absorption spectra of $[\text{Co}(\text{tacn})(\text{aeaps})]^{3+}$ (full) and $[\text{Co}(\text{tacn})(\text{C-aeaps})]^{2+}$ (broken) measured in 1 M NaClO_4 at 25°C .

X-Ray crystallography. The crystals of $[\text{Co}(\text{tacn})(\text{aeaps})](\text{ClO}_4)_3$ and of $[\text{Co}(\text{tacn})(\text{C-aeaps})](\text{ClO}_4)_2$ were characterized at room temperature by Weissenberg photographs. They showed that the crystals belong to the orthorhombic crystal system. They exhibit the same type of absent reflections: $0kl$, $k = 2n + 1$; $h0l$, $l = 2n + 1$; $hk0$, $h = 2n + 1$, which is consistent with the space group $Pbca$. The crystals of $[\text{Co}(\text{tacn})(\text{C-aeaps})](\text{ClO}_4)_2$ were of very poor quality, as shown by the resolution and width of the reflections in the diffraction pattern. Other salts (e.g. the chloride or dithionate) were also examined, but their quality was even poorer.

A CAD4 diffractometer equipped with an Enraf-Nonius gas-flow low-temperature device was used for the data collection. Graphite monochromatized $\text{MoK}\alpha$ radiation was employed. The temperature (ca. 110 K) was monitored with a thermocouple placed a few cm above the crystal in the exhaust pipe. It remained constant within $\pm 0.5 \text{ K}$ during the data collection. The intensities of three standard reflections were monitored every 10 ks, and the orientation of the crystal was checked after every 300 reflections. No deterioration or mis-setting of the crystals was observed.

The selections of scan type and range were based on analysis of the reflection profiles. The crystal data and a summary of data collection parameters and refinement results are listed in Table 3.

Data reduction included corrections for Lorentz and polarization effects and, in the case of $[\text{Co}(\text{tacn})(\text{aeaps})](\text{ClO}_4)_3$, also for absorption. The latter was performed using the Gaussian integration procedure. The symmetry-related reflections were averaged. The two crystal structures were solved by Patterson and Fourier methods and refined by least-squares minimization of $\sum w(|F_o| - |F_c|)^2$.

The crystal structure determination and refinement of $[\text{Co}(\text{tacn})(\text{aeaps})](\text{ClO}_4)_3$ proceeded without any difficulties. The positions of the hydrogen atoms were shown clearly in the difference Fourier calculated after an anisotropic refinement. Their positional parameters were also included in the refinement and they were given a fixed isotropic thermal parameter of 2.50 \AA^2 . The maximum shift after the final cycle was 0.4σ . The residual density had values between 1.39 and $-0.633 \text{ e \AA}^{-3}$. The final atomic parameters are given in Table 4.

The refinement of $[\text{Co}(\text{tacn})(\text{C-aeaps})](\text{ClO}_4)_2$ was not so straightforward. Early in the refinement the difference density suggested that a single chain of the C-aeaps ligand could not account for the electron density in the crystal. It was also evident that one of the perchlorate ions is disordered. An analysis of partly populated atoms that had been introduced showed that they are consistent with two different configurations of the C-aeaps ligand shown for the two cations in Fig. 4. The refined values of the population parameters of C31/S1A and C32A/S2A were identical within two standard deviations and their sum close to 1.0. The population parameter for C31A/S1A and C32A/S2A were averaged and scaled to give the sum 1.00. Similarly

Table 2. Thermodynamic parameters for deprotonation of coordinated amines at 25 °C [eqn. (2)].^a

Complex	Medium	K_b/M	$\Delta H^\circ/kJ\ mol^{-1}$	$\Delta S^\circ/J\ mol^{-1}\ K^{-1}$
[Co(tacn)] ₂ ³⁺	1 M Na(OH,ClO ₄)	1.08(30)		
[Co(tacn)(aeaps)] ³⁺	1 M Na(OH,ClO ₄)	0.433(13)	-19.7(9)	-73(3)
[Co(tacn)(aeaps)] ³⁺	5 M Na(OH,NO ₃)	2.38(22)		
[Co(tacn)(daes)] ³⁺	1 M Na(OH,ClO ₄)	0.505(15)		
[Co(tacn)(C-aeaps)] ²⁺	1 M Na(OH,ClO ₄)	>10		

^aStandard deviations given in parentheses are in units of the last digit.

the sum of the population parameters for oxygen atoms around Cl2 was introduced and scaled to give 1 in the final refinement cycles. Hydrogen atoms were introduced in idealized positions with $B_{iso} = 5.0\ \text{\AA}^2$. The hydrogen atoms bonded to C2A and C4A are, within the experimental accuracy, found to be the same positions for both conformations of the C-aeaps ligands, so only the idealized positions for the more populated conformation was used. The largest peak in the residual density ($1.3\ e\ \text{\AA}^{-3}$) was found close to the disordered perchlorate ion. The final atomic parameters are listed in Table 5. The SDP system was used for the crystallographic computations.¹⁰ The atomic scattering factors and the anomalous dispersion corrections¹¹ were from Ref. 11 and were used as contained in the program. Anisotropic thermal parameters, hydrogen-atom positions and a list of observed and calculated structure amplitudes can be obtained from one of the authors (S.L.).

Results and discussion

Syntheses. The coordination compound [Co(tacn)Cl₃] was

reacted with di(2-aminoethyl)sulfide and 2-aminoethyl-3-aminopropylsulfide to give [Co(tacn)(daes)]Cl₃ and [Co(tacn)(aeaps)]Cl₃, which were isolated as crystalline salts. In aqueous solutions both compounds react fast with strong base to give reddish-purple conjugate base forms as described later. This initial acid–base reaction of [Co(tacn)(aeaps)]³⁺ is followed by a slow reaction which at high base concentration produces the carbon–cobalt bonded complex as shown in Scheme 3. [Co(tacn)(C-aeaps)](ClO₄)₂ was isolated in high yield. A detailed analysis of the thermodynamics and kinetics for the reaction between the sulfur and the carbon bonded species will be reported in a later paper.¹²

The base constants for the reactions have been determined (next section) and are compared to pK_b values for similar systems. ¹³C NMR and ⁵⁹Co NMR have been useful in following the formation of the coordinated carbanion, and this technique has also been used to study the reformation of the coordinated thioether on addition of acid as well as the hydrogen exchange on C4 of the 3-thia-1,6-hexanediamine.¹² The reversibility of the reaction allows us to

Table 3. Crystal data and a summary of data reduction and structure refinement.

Compound	[Co(tacn)(aeaps)](ClO ₄) ₃	[Co(tacn)(C-aeaps)](ClO ₄) ₂
Formula	CoC ₁₁ H ₂₉ Cl ₃ N ₅ O ₁₂ S	CoC ₁₁ H ₂₈ Cl ₂ N ₅ O ₈ S
Formula mass/g mol ⁻¹	620.74	520.27
Space group	<i>Pbca</i>	<i>Pbca</i>
Wavelength (MoK α)/ \AA	0.71073	0.71073
Unit cell dimensions at 110 K:		
<i>a</i> / \AA	28.094(4)	18.169(5)
<i>b</i> / \AA	10.580(3)	15.824(4)
<i>c</i> / \AA	14.620(1)	13.888(4)
<i>V</i> / \AA^3	4345(2)	3993(3)
<i>Z</i>	8	8
<i>F</i> (000)	2560	2168
<i>D_c</i> /g cm ⁻³	1.898	1.734
μ (MoK α)/cm ⁻¹	13.21	12.76
Crystal size/mm ³	0.25 × 0.18 × 0.14	0.12 × 0.30 × 0.45
Scan mode	ω -2 θ	ω
Scan range, $\Delta\omega$ /°	1.0 + 0.35tan θ	1.3 + 0.35tan θ
θ range/°	1–31	1–25
Octants measured	<i>hkl</i> , $-\mathit{hkl}$ (partly)	<i>hkl</i> , $-\mathit{hkl}$
w^{-1}	$\sigma^2(F) + 0.0006 F ^2$	$\sigma^2(F) + 0.0009 F ^2$
$S = \{\sum w \Delta F^2 / (n - m)\}^{1/2}$	1.6	2.1
No. of independent reflections	6918	3503
No. of observed reflections, <i>n</i>	3590	1400
No. of variables, <i>m</i>	385	259
<i>R</i>	0.042	0.074
<i>R_w</i>	0.059	0.096

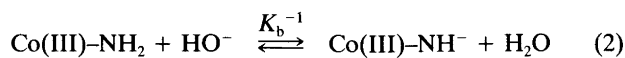
Table 4. Fractional coordinates and equivalent isotropic parameters for [Co(tacn)(aeaps)](ClO₄)₃.

Atom	<i>x/a</i>	<i>y/b</i>	<i>z/c</i>	<i>B/Å</i> ²
Co	0.87781(2)	0.02683(6)	0.22125(4)	0.591(8)
N1A	0.9327(2)	0.1428(4)	0.2007(2)	0.96(7)
C1A	0.9806(2)	0.0824(5)	0.2023(3)	1.28(8)
C2A	0.9831(2)	-0.0148(5)	0.2774(3)	1.46(8)
S	0.93179(4)	-0.1180(1)	0.26364(8)	0.98(2)
C3A	0.9198(2)	-0.1700(5)	0.3793(3)	1.29(9)
C4A	0.9096(2)	-0.0673(5)	0.4485(3)	1.21(8)
C5A	0.8653(2)	0.0100(4)	0.4296(3)	0.98(7)
N2A	0.8703(1)	0.0942(4)	0.3486(2)	0.92(7)
N1B	0.8242(1)	-0.0906(4)	0.2338(3)	0.87(6)
C2B	0.7808(2)	-0.0131(4)	0.2526(3)	0.99(7)
C1B	0.7806(2)	0.0965(5)	0.1863(3)	1.17(8)
N3B	0.8306(1)	0.1484(4)	0.1761(3)	1.00(7)
C3B	0.8187(2)	-0.1723(4)	0.1501(3)	0.97(8)
C4B	0.8630(2)	-0.1648(5)	0.0919(3)	1.25(8)
N2B	0.8805(1)	-0.0313(4)	0.0924(2)	0.87(6)
C5B	0.8506(2)	0.0529(5)	0.0313(3)	1.25(8)
C6B	0.8424(2)	0.1766(5)	0.0783(3)	1.19(8)
Cl1	0.24138(4)	0.2271(1)	0.07892(7)	0.92(2)
O11	0.2824(1)	0.2643(3)	0.1330(2)	1.60(6)
O12	0.2295(1)	0.3261(3)	0.0151(2)	1.50(6)
O13	0.2012(1)	0.2056(3)	0.1389(2)	1.64(7)
O14	0.2527(1)	0.1129(3)	0.0303(2)	1.37(6)
Cl2	0.97933(4)	0.3009(1)	0.45583(7)	1.15(2)
O21	0.9626(2)	0.2461(4)	0.3719(3)	2.75(8)
O22	1.0297(1)	0.3186(3)	0.4497(3)	1.74(7)
O23	0.9684(2)	0.2171(4)	0.5301(3)	2.72(8)
O24	0.9559(1)	0.4207(4)	0.4706(3)	2.42(8)
Cl3	1.12614(4)	-0.0271(1)	0.28489(7)	1.16(2)
O31	1.0907(1)	-0.0672(4)	0.3503(2)	1.82(7)
O32	1.1700(2)	-0.0048(5)	0.3316(3)	3.2(1)
O33	1.1319(2)	-0.1277(4)	0.2191(3)	2.58(8)
O34	1.1101(2)	0.0847(4)	0.2398(3)	2.78(9)

determine the equilibrium quotient for the equation in Scheme 3 by spectrophotometry and HPLC methods, and the results are seen in structural perspectives in view of the results of the crystal structure determinations.

Deprotonation of coordinated amines. Addition of base to an aqueous solution of [Co(tacn)(aeaps)]Cl₃ · H₂O gives an instantaneous change in colour from yellow–brown to reddish–purple for ca. pH 14 or greater. The reaction is reversible and the [Co(tacn)(aeaps)]³⁺ cation is re-formed, also instantaneously, when e.g. an excess of NH₄Cl is added to a freshly prepared basic solution (shown using VIS spectroscopy and by HPLC). Visually it was estimated that the reaction has *t*_{1/2} < 1 s at 0 °C, and stopped-flow measurements confirmed this estimate and showed that *t*_{1/2} < 10 ms at 25 °C. It therefore seems reasonable to interpret this reaction as an ordinary acid–base reaction involving deprotonation of a coordinated secondary amine group in the 1,4,7-triazacyclononane or a primary amine in the aeaps ligand. The acid–base equilibrium was studied spectrophotometrically at three different temperatures using *I* = 1.0 M Na(ClO₄, OH) as described in detail in the Experimental section. The variation of the spectra with the

hydroxide concentration could be interpreted in terms of a single acid–base reaction [eqn. (2)], and its equilibrium



constant was determined by non-linear regression analysis. From Fig. 1 it is seen that there is good agreement between the calculated and observed ϵ -values. The equilibrium constant K_b is well defined, as seen in Table 2. The calculated spectrum of the basic form, [Co(tacn)(aeaps-N⁻)]²⁺, is shown in Fig. 2. From the temperature dependence of K_b the values of ΔS° and ΔH° were obtained (Table 2). Measurements at higher ionic strength gave results of the same order of magnitude (Table 2). It was found that [Co(tacn)₂]³⁺ and [Co(tacn)(daes)]³⁺ also react instantaneously and reversibly with base, and their K_b values were determined likewise (Fig. 2 and Table 2). Similar studies of the acid–base properties of the alkyl complex showed that the cation does not deprotonate to any measureable extent in 1 M NaOH at 25 °C (¹³C NMR and UV–VIS spectroscopy), and this supports the estimate that $K_b > 10$.

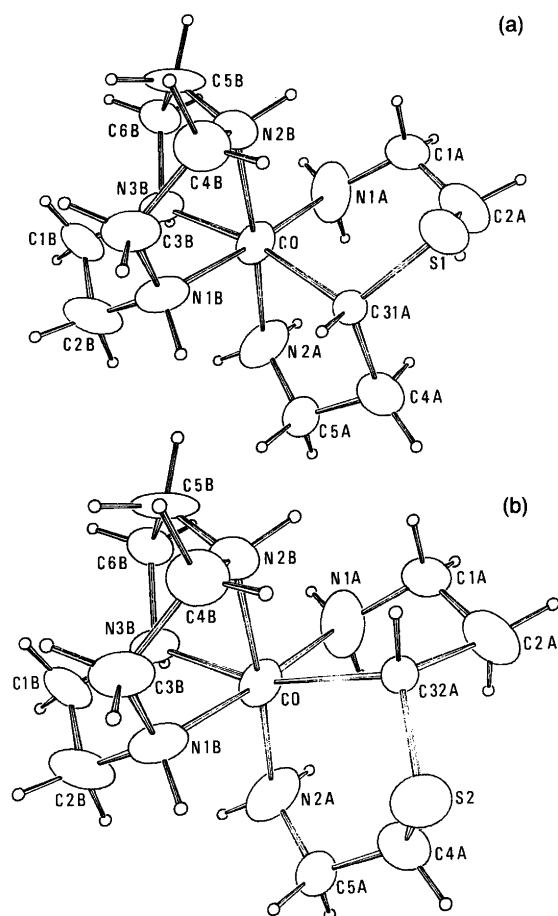


Fig. 4. The two different configurations of the cation [Co(tacn)(C-aeaps)]²⁺ which occupy the crystal, with their atomic labelling. The thermal ellipsoids are scaled to include 50% probability, and the hydrogen atoms are drawn as spheres with a fixed radius.

Table 5. Fractional coordinates and equivalent isotropic parameters for $[\text{Co}(\text{tacn})(\text{C-aeaps})](\text{ClO}_4)_2$.^a

Atom	<i>x/a</i>	<i>y/b</i>	<i>z/c</i>	<i>B</i> _{iso} /Å
Co	0.87276(9)	0.0767(1)	0.2024(1)	4.20(3)
N1A	0.9781(6)	0.112(1)	0.2037(9)	7.6(4)
C1A	1.0062(7)	0.1646(8)	0.284(1)	5.0(3)
C2A	0.9879(9)	0.126(1)	0.379(1)	7.6(5)
S1 (0.65)	0.8980(4)	0.1284(4)	0.4183(4)	5.4(1)
C31A (0.65)	0.8643(2)	0.048(1)	0.346(1)	3.0(3) ^b
C32A (0.35)	0.894(2)	0.108(2)	0.350(2)	2.9(6) ^b
S2 (0.35)	0.8492(6)	0.0289(8)	0.4181(9)	6.0(3)
C4A	0.9005(8)	-0.0471(9)	0.366(1)	5.4(3)
C5A	0.8809(7)	-0.0941(8)	0.2799(9)	4.4(3)
N2A	0.9008(7)	-0.0448(8)	0.1961(9)	7.0(3)
C1B	0.7899(8)	0.0571(9)	0.027(1)	6.5(4)
C2B	0.756(1)	0.0058(9)	0.102(1)	7.2(4)
N1B	0.7682(6)	0.0491(6)	0.1955(8)	4.8(3)
C3B	0.7222(8)	0.1222(8)	0.213(1)	5.7(4)
C4B	0.7639(7)	0.1939(8)	0.248(1)	5.5(4)
N2B	0.8367(5)	0.1939(6)	0.2032(8)	4.4(2)
C5B	0.8367(9)	0.2289(7)	0.109(1)	6.4(4)
C6B	0.8747(7)	0.1805(8)	0.034(1)	5.2(3)
N3B	0.8648(6)	0.0873(6)	0.0559(8)	4.7(2)
Cl1	1.1207(2)	0.1906(3)	0.0143(3)	5.81(9)
O11	1.1306(6)	0.2143(7)	-0.0799(8)	7.2(3)
O12	1.079(1)	0.106(1)	0.007(1)	15.9(6)
O13	1.0676(7)	0.2309(8)	0.066(1)	13.7(4)
O14	1.1794(8)	0.150(1)	0.048(1)	15.6(6)
Cl2	1.1043(2)	-0.0853(2)	0.2252(3)	4.61(7)
O21	1.1796(4)	-0.1042(6)	0.2107(8)	5.8(2)
O22	1.0946(6)	-0.0305(9)	0.300(1)	10.8(4)
O23A (0.50)	0.9318(9)	0.159(1)	0.798(1)	4.7(4) ^b
O23B (0.5)	0.935(1)	0.149(1)	0.711(1)	5.4(4) ^b
O24A (0.50)	1.0867(9)	-0.021(1)	0.146(1)	4.9(4) ^b
O24B (0.50)	1.060(1)	-0.076(1)	0.144(1)	5.6(4) ^b

^aPopulation parameters different from 1.0 are given in parentheses. ^bAtoms refined isotropically.

The observation that $[\text{Co}(\text{tacn})_2]^{3+}$ ($\text{p}K_a = 13.83$) is a weaker acid than $[\text{Co}(\text{tacn})(\text{aeaps})]^{3+}$ ($\text{p}K_a = 13.44$) is contrary to the expectation based upon the acidities of Me_3NH^+ ($\text{p}K_a = 9.8$) and Me_2NH_2^+ ($\text{p}K_a = 10.8$).¹³ This could be due to different hydrations of the two species, although it cannot be excluded that deprotonation of the $[\text{Co}(\text{tacn})(\text{aeaps})]^{3+}$ cation takes place (predominantly) at the amine groups of the aeaps ligands, and not at the tacn ligand as expected. The $\text{p}K_a$ value for $[\text{Co}(\text{tacn})_2]^{3+}$ is significantly smaller than that reported for $[\text{Co}(\text{en})_3]^{3+}$ ($\text{p}K_a > 14$),¹⁴ as one would expect following the lines above. Hexaaminocobalt(III) cage complexes have also been reported to form amido complexes in aqueous solution, with $\text{p}K_a$ values of about 10.¹⁵ The observation that secondary amines in cage complexes are more acidic than those of, e.g., 1,4,7-triazacyclononane is in agreement with the more hydrophobic character of the former species.

The lower acidity of the alkyl complex as compared with that of the corresponding sulfur-bonded species is probably due to the different charges of the species.

NMR results. The ¹³C DEPT NMR spectrum of a 0.2 M solution of $[\text{Co}(\text{tacn})(\text{aeaps})]^{3+}$ in D₂O is shown in Fig. 5A. The spectrum contains 11 resonance signals as expected, because this cation contains no symmetry elements.

The chemical shift signals of ligand atoms in coordination compounds are usefully discussed in terms of the coordination shift, defined as the difference in shielding from the free to the coordinated ligand. The ¹³C signals of nitrogen- and sulfur-containing organic ligands coordinated to Co(III) have small coordination shifts, typically less than 10 ppm, and may be of either sign. However, general trends for the coordination shifts have been noticed from the ¹³C NMR spectra of numerous Co(III) coordination compounds with organic ligands containing nitrogen and sulfur donor atoms in five- and six-membered chelate rings.⁶ It was noticed that carbon adjacent to nitrogen or sulfur in a five-membered chelate ring displays a small positive shift change on coordination, whereas carbon neighbouring nitrogen in a six-membered chelate ring has a signal with a negligible shift change. The signal from the middle carbon atom in a six-membered chelate ring has a large negative shift on coordination.⁶ Based on these findings the six resonances at higher frequency in Fig. 5A are attributed to the six carbon atoms in the tacn ligand, and the remaining five resonance lines have been assigned accordingly to com-

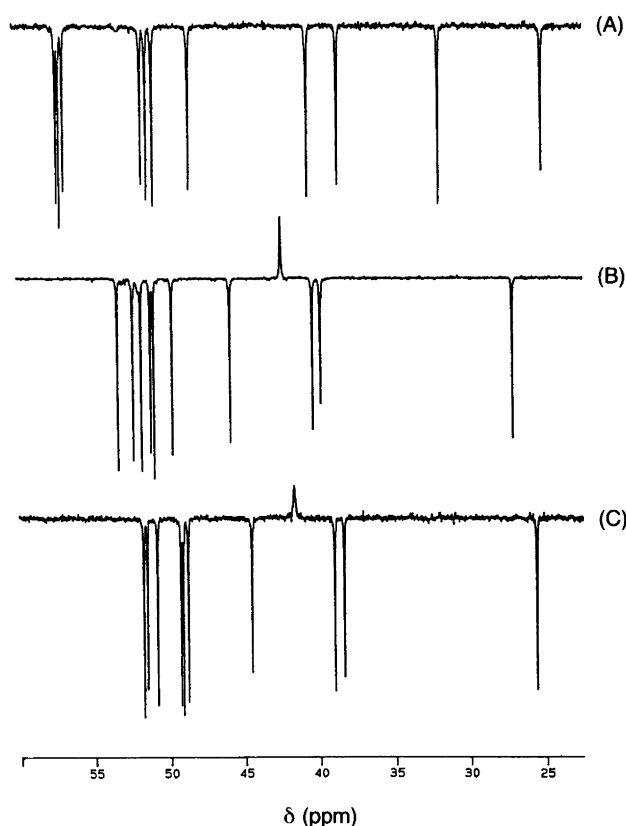


Fig. 5. ¹³C NMR spectra. (A) $[\text{Co}(\text{tacn})(\text{aeaps})]\text{Cl}_3$ in D₂O. (B) $[\text{Co}(\text{tacn})(\text{C-aeaps})]^{2+}$ in 1 M NaOD (see text). (C) $[\text{Co}(\text{tacn})(\text{C-aeaps})](\text{ClO}_4)_2$ in acetonitrile-d₃. All spectra were measured at 300 K.

Table 6. ^{13}C NMR δ -values for cobalt(III) coordination compounds with tacn and aeaps.^a

Compound	tacn						aeaps, numbering of atoms				
	1	2	4	5	6		1	2	4	5	6
tacn · 3HCl	43.7										
[Co(tacn) ₂]Cl ₃	53.0										
aeaps							42.2	36.5	30.8	34.2	42.0
[Co(tacn)(aeaps)]Cl ₃	57.2	57.0	56.7	51.5	51.1	50.7	48.4	38.5	31.8	25.0	40.5
[Co(tacn)(C-aeaps)](ClO ₄) ₂	53.4	52.4	51.8	51.2	51.1	49.8	40.4	27.1	42.6	39.9	45.9
[Co(tacn)(C-aeaps)](ClO ₄) ₂ ^b	50.8	49.0	48.9	48.7	48.5	46.3	37.7	24.6	38.1	36.7	42.9
[Co(tacn)(C-aeaps)](ClO ₄) ₂ ^c	51.7	51.5	50.8	49.3	49.1	48.8	39.0	25.6	41.6	38.4	44.5

^aThe aeaps ligand is numbered N–C1–C2–S–C4–C5–C6–N in accordance with the name 3-thia-1,6-hexanediamine. Notice the different numbering in the crystallographic results. ^bIn DMSO-d₆. ^cIn acetonitrile-d₃. All others in D₂O.

ply with the above general coordination shifts. The data are collected in Tables 6 and 7.

The ^{59}Co NMR spectrum of [Co(tacn)(aeaps)](ClO₄)₃ in acetonitrile at 330 K is shown in Fig. 6, and it is seen to display a relatively narrow resonance line ($\Delta\nu_{1/2} = 344$ Hz) at 6456 ppm. The relatively narrow line demonstrates that the electric field gradient is small (*vide infra*), and it means that thioether coordinates to cobalt(III) with approximately the same charge transfer as does an amine.

The ^{13}C DEPT NMR spectrum of 0.2 M [Co(tacn)(C-aeaps)]²⁺ in 1 M NaOD is shown in Fig. 5B. This sample was made by adding a solution of NaOD to a solution of [Co(tacn)(aeaps)]³⁺ in D₂O, and spectral collection was commenced after 48 h. Since the resonance signal at 42.60 ppm is the only one that is positive, it is assigned to the cobalt-bound carbon atom, as this is the only possible CH group. The existence of a CH group is direct evidence that the alkyl compound exists in aqueous solution.

The existence of the CH group was confirmed by using $\theta = \pi/2$ in the DEPT pulse sequence. This experiment suppresses all other ^{13}C NMR signals than those from CH groups.

Table 7. Assignment of ^{13}C chemical shift (δ -values) for [Co(tacn)(aeaps)]³⁺ (a) and [Co(tacn)(C-aeaps)]²⁺ (b) based on changes ($\Delta\delta$) occurring on coordination.

C No.	δ (free) (ppm)	δ (bound) (ppm)	Coordination shift ($\Delta\delta$ /ppm)	Expected range ($\Delta\delta$ /ppm)
(a)				
1	42.2	48.4	6.2	5±5
2	36.5	38.5	2.0	3±2
4	30.8	31.8	1.0	–
5	34.2	25.0	–9.2	–9±2
6	42.0	40.5	–1.5	0±1
(b)				
1	42.2	40.4	–1.8	0±1
2	36.5	27.1	–9.4	–9±2
4	30.8	42.6	11.8	–
5	34.2	39.9	5.7	–
6	42.0	45.9	3.9	5±5

Provided that the above rules for coordination shifts are also valid for the non-coordinating carbon atoms in a chelate alkyl cobalt(III) compound, an assignment of the four remaining carbon resonance signals from the aeaps ligand may be made. The only difference is that the five- and six-membered rings are interchanged on going to the alkyl compound from the sulfur-bound complex. This assignment is also given in Table 6, and the coordination shifts obtained by the assignment are shown in Table 7.

The ^{13}C DEPT NMR spectrum of [Co(tacn)(C-aeaps)](ClO₄)₂ in acetonitrile-d₃ (Fig. 5C) exhibits the same pattern as the spectrum obtained in D₂O (Fig. 5A), and the resonance signals may be assigned in the same manner. In particular, the spectrum displays a CH group. This confirms the existence of an alkyl compound in solution, since hydrolysis reactions can be excluded.

The ^{59}Co NMR spectrum of [Co(tacn)(C-aeaps)](ClO₄)₂ in acetonitrile at 330 K displays a very broad line ($\Delta\nu_{1/2} = 12\,480$ Hz) at 6540 ppm (Fig. 6). The resonance line is

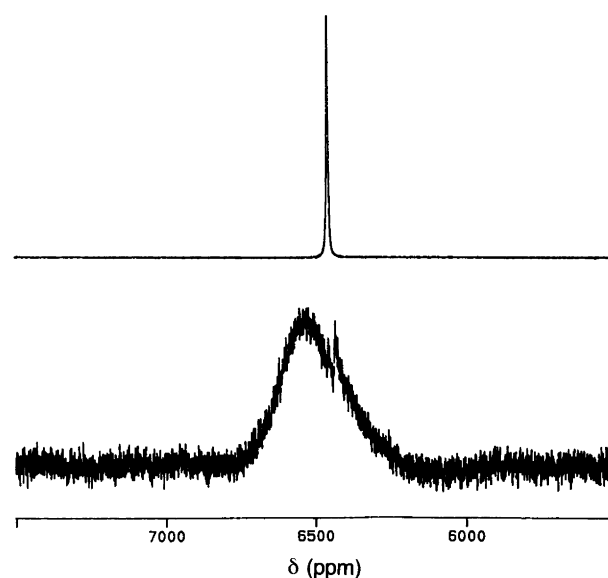


Fig. 6. ^{59}Co NMR spectra. [Co(tacn)(aeaps)](ClO₄)₃ in acetonitrile at 330 K (top) and [Co(tacn)(C-aeaps)](ClO₄)₂ in acetonitrile at 330 K (bottom).

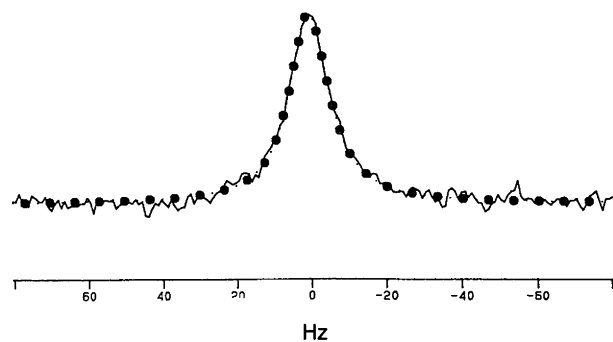


Fig. 7. The ^{13}C NMR signal for the cobalt-bound carbon atom in $[\text{Co}(\text{tacn})(\text{C-aeaps})](\text{ClO}_4)_2$ in acetonitrile- d_1 at 330 K (solid line). The dotted line is the line-shape calculated for $T_{1,\text{Co}} = 2.55 \times 10^{-5}$ s and $^1J_{\text{Co-C}} = 86$ Hz.

broader at lower temperatures, and it is broadened beyond detection in aqueous solution. Note that there is a 36-fold increase in linewidth compared to the compound with the thioether coordinating. This reflects a similar increase of the electric field gradient, if the two compounds have identical rotational correlation times. Since they only differ by one proton we consider this condition obeyed.

There is only a small ^{59}Co chemical shift difference in the signals from $[\text{Co}(\text{tacn})(\text{aeaps})](\text{ClO}_4)_3$ and $[\text{Co}(\text{tacn})(\text{C-aeaps})](\text{ClO}_4)_2$. This may be compared with the position of the first absorption band of the visible absorption spectra of the two compounds: $\lambda_{\text{max}} = 476$ nm, $\epsilon_{\text{max}} = 126 \text{ dm}^3 \text{ mol}^{-1} \text{ cm}^{-1}$ for $[\text{Co}(\text{tacn})(\text{aeaps})]^{3+}$ and $\lambda_{\text{max}} = 464$ nm, $\epsilon_{\text{max}} = 95 \text{ dm}^3 \text{ mol}^{-1} \text{ cm}^{-1}$ for $[\text{Co}(\text{tacn})(\text{C-aeaps})]^{2+}$. The corresponding absorption feature for $[\text{Co}(\text{tacn})_2]^{3+}$ is $\lambda_{\text{max}} = 460$ nm and $\epsilon_{\text{max}} = 95 \text{ dm}^3 \text{ mol}^{-1} \text{ cm}^{-1}$. Thus, the carbanion ligand has ligand field properties relatively similar to those of an amine.

^{13}C – ^{59}Co coupling constants. The ^{59}Co nucleus has nuclear spin $I = 7/2$, and hence one might expect a splitting of the ^{13}C NMR signal of the cobalt-bound carbon atom into eight lines owing to scalar coupling. However, the relaxation rate of the ^{59}Co nucleus may be so fast that the eight lines will collapse into a single line at the centre of the multiplet. ^{59}Co has a large quadrupole moment ($Q = 38 \times 10^{-30} \text{ m}^2$) which interacts with the electric field gradient at the site of the nucleus. The quadrupole interaction is proportional to both the nuclear quadrupole moment and the electric field gradient, and the quadrupole interaction causes transitions between the magnetic states of the ^{59}Co nucleus, leading to fast relaxation of these states. In this case scalar coupling between the ^{59}Co nucleus and the ^{13}C nucleus contributes to the spin–spin relaxation rate of the ^{13}C nucleus. Therefore the ^{13}C NMR signal of the cobalt-bound carbon is broad compared to the other signals. From the linewidth and the spin–lattice relaxation time, T_1 , of the quadrupolar nucleus the coupling constant, J , may be approximately extracted despite the absence of a direct splitting.

The linewidth of the ^{13}C signal for the cobalt-bound carbon is considerably larger in acetonitrile than in D_2O . This is attributed to the difference in viscosity. Acetonitrile is a less viscous solvent than water, and therefore the ^{59}Co spin–lattice relaxation time is longer in acetonitrile. When a solution of $[\text{Co}(\text{tacn})(\text{C-aeaps})](\text{ClO}_4)_2$ in acetonitrile is heated from 300 to 330 K all ^{13}C resonance lines become narrower, except that of the cobalt-bound carbon, which becomes wider, as heating decreases the rotational correlation time of the molecule. Consequently, T_1 of the ^{59}Co nucleus increases, resulting in a broader ^{13}C resonance line of the cobalt-bound carbon. At 330 K this signal has a linewidth of $\Delta\nu_{1/2} = 12.6$ Hz (Table 8). For comparison the linewidths of the other ^{13}C NMR signals are about 0.5 Hz.

The ^{13}C NMR lineshape of the cobalt-bound carbon may be calculated using a relaxation matrix treatment developed by Pyper¹⁶ if the ^{59}Co nucleus relaxes solely due to a quadrupole interaction. The spin–lattice relaxation time, T_1 , for the cobalt nucleus can be obtained from the linewidth of the ^{59}Co NMR spectrum (Fig. 6 and Table 8). Using this T_1 -value for the cobalt nucleus, $J_{\text{Co-C}}$ may be varied in a calculation of the line-shape of the ^{13}C resonance of the cobalt-bound carbon until good agreement with the experimental resonance line is given (Fig. 7). In this way the carbon–cobalt coupling constant was calculated to be $^1J_{\text{Co-C}} = 86$ Hz (Table 8). If the line-shape of the ^{13}C NMR line receives a significant contribution from mechanisms other than scalar coupling to cobalt this would lead to a computed value for the coupling constant that is too high. However, since the scalar coupling constant contains important information about the nature of the chemical bond, it is fortunate to be able to obtain an estimate of the maximum size of J .

For comparison we have measured the ^{59}Co NMR and ^{13}C NMR spectra of methyl- and ethylcobaloxime (prepared according to Schrauzer)¹⁷ in CHCl_3 at 300 K, and likewise compared the experimental and calculated line-shapes to extract $^1J_{\text{Co-C}}$. The results are given in Table 8. The uncertainty of the calculated coupling constants has been estimated to be ± 5 Hz.

The coupling constants $^1J_{\text{Co-C}}$ in these compounds are calculated to be almost constant despite the large variations in linewidths, and this seems to support the validity of the results.

Table 8. Single-bond cobalt–carbon coupling constants $^1J_{\text{Co-C}}$ obtained by simulation of the line-shape of the ^{13}C NMR signal.

Complex	^{59}Co NMR		^{13}C NMR	
	$\Delta\nu_{1/2}/\text{Hz}$	$10^5 T_1/\text{s}$	$\Delta\nu_{1/2}/\text{Hz}$	$^1J_{\text{Co-C}}/\text{Hz}$
$[\text{Co}(\text{tacn})(\text{C-aeaps})]^{2+}$ ^a	12480	2.55	12.6	86
Methyl(pyridine)cobaloxime ^b	6396	4.98	20.6	79
Ethyl(pyridine)cobaloxime ^b	5565	5.72	25.5	82

^aIn acetonitrile at 330 K. ^bIn CHCl_3 at 300 K.

Table 9. Comparisons of $^1J_{\text{Co-C}}$ and $^1J_{\text{Rh-C}}$.

Species	Ref.	$^1J_{\text{metal-C}}/\text{Hz}$	$J_{\text{Co-C}}/J_{\text{Rh-C}}$
$[\text{Co}(\text{CN})_6]^{3-}$	16	126	3.75
$[\text{Rh}(\text{CN})_6]^{3-}$	16	33.6	
$[\text{Co}(\text{CO})_4]^-$	17	287	3.84
$[\text{Rh}(\text{CO})_4]^-$	17	74.7	
Alkyl cobalt(III)	—	79–86	≈ 3.8
Alkyl rhodium(III)	17	17–26	

To our knowledge only cobalt–carbon coupling constants for hexacyanocobaltate(III) and tetracarbonylcobaltate(-1) have been reported. Both these compounds have cubic symmetry, and the coupling constants may be read directly from the splittings of the spectra. The coupling constants reported in this article are smaller than those of the two abovementioned compounds. This is expected, since the alkyl cobalt(III) compounds contain a pure single bond and so have no contributions from π -bonding to the coupling constant.

The calculated coupling constants may also be compared to rhodium–carbon coupling constants. For a certain type of chemical bond an approximately constant ratio between $^1J_{\text{Co-C}}$ and $^1J_{\text{Rh-C}}$ could be predicted. For alkyl rhodium(III) compounds $^1J_{\text{Rh-C}}$ are generally about 20 Hz (Table 9). Therefore, using the data of Table 9 one would anticipate a value of $^1J_{\text{Co-C}}$ of about 80 Hz, which is in agreement with the experimental findings.

All these data thus substantiate the presence of a carbon–cobalt(III) bond in solution.

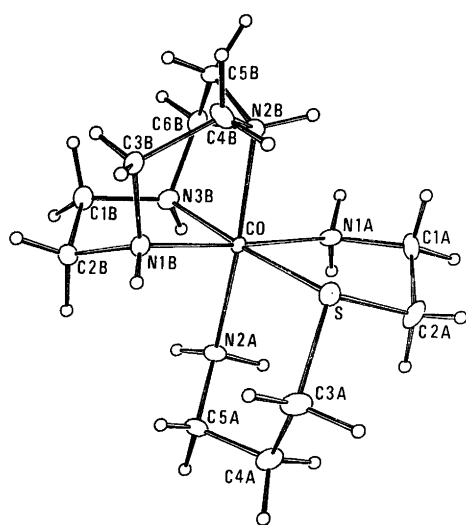


Fig. 8. The molecular structure of $[\text{Co}(\text{tacn})(\text{aeaps})]^{3+}$ showing the atomic numbering. The thermal ellipsoids are scaled to include 50% probability, and the hydrogen atoms are drawn as spheres with a fixed radius.

Table 10. Selected bond distances, D , and angles, α , for the two cations.

	$[\text{Co}(\text{tacn})(\text{aeaps})]^{3+}$	$[\text{Co}(\text{tacn})(\text{C-aeaps})]^{2+}$
	$D/\text{\AA}$	$D/\text{\AA}$
Co–N1A	1.994(4)	1.992(11)
Co–N2A	2.004(4)	1.992(11)
Co–S/C31A	2.2433(13)	2.05(2)
Co–N1B	1.960(4)	1.951(9)
Co–N2B	1.984(3)	1.966(9)
Co–N3B	1.965(4)	2.047(10)
N1A–C1A	1.491(7)	1.48(2)
C1A–C2A	1.506(7)	1.49(2)
C2A–S	1.819(5)	1.73(2)
S–C3A	1.810(5)	1.73(2)
C3A–C4A	1.512(7)	1.67(2)
C4A–C5A	1.515(7)	1.46(2)
C5A–N2A	1.489(6)	1.45(2)
N1B–C2B	1.494(6)	1.48(2)
C2B–C1B	1.512(7)	1.46(2)
C1B–N3B	1.511(6)	1.499(14)
N1B–C3B	1.506(6)	1.449(13)
C3B–C4B	1.511(7)	1.45(2)
C4B–N2B	1.495(6)	1.465(13)
N2B–C5B	1.516(6)	1.42(2)
C5B–C6B	1.496(7)	1.46(2)
C6B–N3B	1.499(6)	1.515(14)
	$\alpha/1^\circ$	$\alpha/1^\circ$
N1A–Co–N2A	90.2(2)	91.3(5)
N1A–Co–S/C3A	86.52(12)	97.1(6)
N1A–Co–N1B	176.6(2)	176.1(5)
N1A–Co–N2B	91.1(2)	93.3(4)
N1A–Co–N3B	94.1(2)	93.1(4)
S/C3A–Co–N2A	93.31(12)	81.3(5)
S/C3A–Co–N1B	93.45(12)	85.7(5)
S/C3A–Co–N2B	91.43(12)	100.2(5)
S/C3A–Co–N3B	176.22(12)	168.4(5)
N2A–Co–N1B	93.3(2)	91.8(4)
N2A–Co–N2B	175.2(2)	174.9(4)
N2A–Co–N3B	90.4(2)	93.1(4)
N1B–Co–N2B	85.5(2)	83.6(4)
N1B–Co–N3B	85.8(2)	84.3(4)
N2B–Co–N3B	84.8(2)	84.5(4)
N1A–C1A–C2A	110.2(4)	110.6(10)
C1A–C2A–S	107.1(3)	118.90(11)
C2A–S–C3A	103.1(2)	97.5(8)
S–C3A–C4A	116.2(3)	115.1(10)
C3A–C4A–C5A	114.8(4)	103.0(10)
C4A–C5A–N2A	113.0(4)	109.1(10)
N1B–C2B–C1B	107.9(4)	108.1(10)
C2B–N1B–C3B	109.7(4)	111.1(12)
C1B–N3B–C6B	111.9(4)	111.3(9)
N1B–C3B–C4B	110.0(4)	112.3(9)
C3B–C4B–N2B	108.6(4)	109.0(10)
C4B–N2B–C5B	111.7(4)	113.2(10)
N2B–C5B–C6B	109.2(4)	116.6(9)
C5B–C6B–N3B	107.5(4)	108.3(9)

Table 11. Hydrogen-bond distances and angles in [Co(tacn)(aeaps)](ClO₄)₃.

	Distance (D—H...A)/Å	Angle (D—H—A)/°
N1A—HA11N—O23 ^a	3.069(5)	165(5)
N2A—HA21N—O21	3.070(6)	172(5)
N2A—HA22N—O11 ^b	3.067(5)	171(5)
C3A—HA32C—O23 ^c	3.446(7)	152(4)
N1B—HB1—O13 ^d	2.936(5)	157(6)
N2B—HB2—O22 ^e	3.047(5)	136(4)
N2B—HB2—O24 ^a	3.005(5)	129(4)
N3B—HB3—O33 ^f	3.012(5)	172(5)

^a(*x*, -1/2-*y*, -3/2+*z*). ^b(-1/2+*x*, *y*, -1/2-*z*). ^c(2-*x*, -*y*, 1-*z*). ^d(1-*x*, -1/2+*y*, 1/2-*z*). ^e(2-*x*, -1/2+*y*, 1/2-*z*). ^f(2-*x*, 1/2+*y*, 1/2-*z*).

Description of the structures. The molecular geometries of the starting material [Co(tacn)(aeaps)](ClO₄)₃ and the product [Co(tacn)(C-aeaps)](ClO₄)₂ are depicted in Figs. 4 and 8, and the bond lengths, bond and torsion angles are listed in Tables 10 and 11. The conformations and geometries of the tacn ligand are the same in the two structures, indicating that the macrocyclic ligand is not affected by the transformation from sulfur to carbanion coordination. As illustrated in Fig. 4, the disorder of the [Co(tacn)(C-aeaps)]²⁺ ion corresponds to an interchange of the five- and six-membered ring on the same crystallographic site. This disorder would be expected to affect all the atoms of the C-aeaps ligands, but only for C3(1,2) and S(1,2) are the sites sufficiently well resolved to be included in the refinement. From the drawings (Fig. 4) one might believe that the disorder results in a different stereochemistry of the cation, but inspection of the torsion angles reveals that the C-aeaps ligand adopts conformations that are mirror images, so that the coordinating carbon atoms are found to have opposite absolute configuration on the same site. The five-membered rings of the tacn ligands are puckered to achieve the same absolute configuration in the two forms of the disordered cation.

The six-membered rings of the aeaps and C-aeaps ligands are all found in chair conformations. It is unfortunate that the accuracy of the structure of the product does not permit a detailed comparison of the two structures. Considering

that the partly populated atoms are so close that they cannot be well separated owing to the limited resolution of the diffraction data, the molecular geometry of the C-aeaps ligand compares well with that found in the accurately determined structure of [Co(aeaps)(C-aeaps)]S₂O₆.² It should be noted that an elongation of the Co—N bond *trans* to the Co—C bond can also be observed in the present structure, where Co—N3B has a bond distance of 2.05 Å compared to 1.955 Å for the two other Co—N distances involving the tacn ligand.

The structural features of the sulfur-coordinating starting material are similar to those of the analogous compounds [Co(daes)₂]Cl₃·2H₂O¹⁸ and [Co(aeaps)(C-aeaps)]S₂O₆.²

The two structures reported here crystallize in the same orthorhombic space group *Pbca* but with different cell dimensions. However, in both structures the crystal packing is influenced by hydrogen bonds between the perchlorate ions and the complex cations, as illustrated by the stereo pairs of Figs. 9 and 10. It should be emphasised that, based on the criterion that a distance less than 2.4 Å between hydrogen and an acceptor atom is evidence for a hydrogen bond, we find that one proton on C3A (H_a) is involved in a weak interaction (Table 11). The less charged cation [Co(tacn)(C-aeaps)]²⁺ is equally well involved in hydrogen bonding (Table 12), and here a close contact is found between a carbon-bound hydrogen and an oxygen.

Cyclic voltammetry. The observed cyclic voltammograms had peak separations in the range 60–100 mV with sweep rates 5–45 mV s⁻¹. The results were interpreted as reversible electrode reactions with a slight loss of the reduced species at the electrode surface. Thus the ratio between the cathodic and anodic peak currents, *I*_{pc}/*I*_{pa}, varied from 1.51 (45 mV s⁻¹) to 1.43 (5 mV s⁻¹) for [Co(tacn)(aeaps)]³⁺. With sufficiently fast scans we assume the electrode processes to be electrochemically reversible and to provide information on the relative stabilities of the species. The stability of a thioether coordinated to cobalt(III) has earlier been estimated for [Co(daes)₂]³⁺ to be very low.¹⁹ The reduction potentials for aqueous solutions of [Co(tacn)(daes)]³⁺ (*E*^o = -0.18 V) and [Co(tacn)(aeaps)]³⁺ (*E*^o = -0.11 V) indicates that the latter species is the least stable. This is also implied from the fact that [Co(aeaps)₂]³⁺

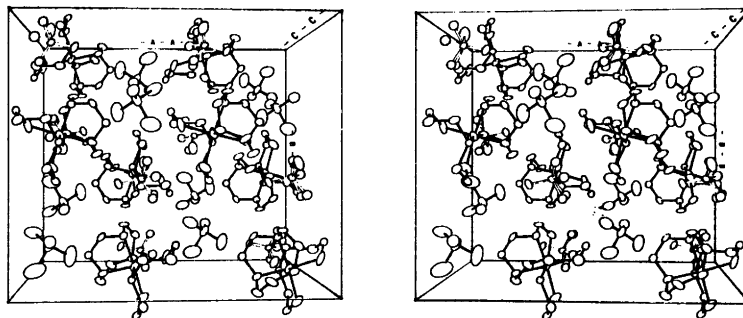


Fig. 9. Stereoscopic drawing of the unit cell for [Co(tacn)(aeaps)](ClO₄)₃ viewed along the *c*-axis, the hydrogen bonds are drawn as thin lines.

Table 12. Short intermolecular interactions, possible hydrogen bonds, in $[\text{Co}(\text{tacn})(\text{C-aeaps})](\text{ClO}_4)_2$.

	Distance (D-H...A)/Å	Angle (D-H-A)/°
N1A-H1N1A...O13	3.37(2)	144
N1A-H2N1A...O24A	3.00(2)	142
N2A-H1N21...O12 ^a	3.00(2)	143
N2A-H2N2A...O24B	3.02(2)	152
N1B-H1N1B...O21 ^b	3.19(12)	147
C5B-H1C5B...O23B ^c	2.99(2)	126
N2B-H1B2B...O23A ^c	3.19(2)	161
N2B-H1B2B...O23B ^c	3.06(2)	136
N3B-H1N3A...O24A	3.12(2)	132
N3B-H1N3B...O24B	3.11(2)	127

^a(2-x, -y, -z). ^b(x-1/2, y, 1/2-z). ^c(x, 1/2-y, z-1/2).

isomers cannot be prepared from aqueous solution.²⁰ The very low reduction potential for $[\text{Co}(\text{tacn})(\text{C-aeaps})]^{2+}$ ($E^{\circ'} = -1.28$ V) in acetonitrile is difficult to compare directly with the values for the thioether-bound compounds. However, we can safely conclude that the alkyl cobalt(III) compound is very stable compared to the cobalt(II) analogue.

Ylide formulation of the reaction. The coordination compound $[\text{Co}(\text{tacn})(\text{aeaps})]^{3+}$ is chiral, having a chiral, coordinated sulfur and a chiral distribution of the five- and six-membered chelate rings of the aeaps ligand. This makes the two hydrogen atoms on C3A prochiral or diastereotopic. Another description of the two hydrogen atoms could be as axial (H_a) or equatorial ($H_e = \text{HA}32\text{C}$) substituents on the six-membered chelate ring. The formation of the alkyl coordination compound according to Scheme 2 has been shown to be a reversible and stereospecific process.¹² Analysis of the diastereotopic relationship between the sulfur- and the carbon-bound ligands in the two structures shows that H_a on C3A is leaving in Scheme 2. A C-H...O interaction with an H...O distance lower than

2.4 Å is often taken as evidence for hydrogen bonding.²¹ The hydrogen atom on C3A that is involved in hydrogen bonding according to Table 11 is not the acid hydrogen that leaves on base addition. From the crystal structure and from ¹H NMR and ¹³C NMR spectroscopy only there are reasons to believe that H_a and H_e have structurally and energetically very similar properties in $[\text{Co}(\text{tacn})(\text{aeaps})]^{3+}$. Therefore, the reason for the stereospecificity is most likely to be found in the two presumably different transition states for the removal of the H_a and H_e protons. When a proton is dissociated from the aeaps ligand it is possible to formulate the base as a coordinated ylide with a resonance formula having a π -bond between sulfur and C3A. The ylide intermediate state (e.g. written as $\text{Co-S}^+(\text{C3A})\text{C}^-\text{H}_e(\text{C4A})\text{H}_2^-$) has a π -bonding molecular orbital made up largely of the sulfur p-orbital pointing toward cobalt and a p-orbital on carbon, C3A, parallel to this sulfur p-orbital. We suppose that this is important for the formation of a precursor in Scheme 3 from structure V to VI. The carbanion formed when H_e has dissociated has no possibility of a similar electronic arrangement. Thus the ylide coordination compound formed after dissociation of H_a is closer in energy to the transition state for the Co-S to Co-C transformation than the ylide derived by removing H_e . The geometry of the proposed π -molecular orbital suggests that it acts as a σ -donor during the transition from the sulfur- to the carbon-bound states. This type of reaction is very different from the C-H activation observed for bis(1,4,7-trithiacyclononane)rhodium(III), which on base addition breaks a sulfur-carbon bond.²² A study of the kinetics of hydrogen exchange of diastereotopic protons in cyclic sulfonium ions has shown that a difference in acidity may be explained by orbital overlap considerations.²³ In that study the observed stereospecificities were much less than in our case, emphasizing both the special orbital overlap arrangement, with a π -orbital donating to a d_σ -orbital, and the high steric rigidity implied by chelation.

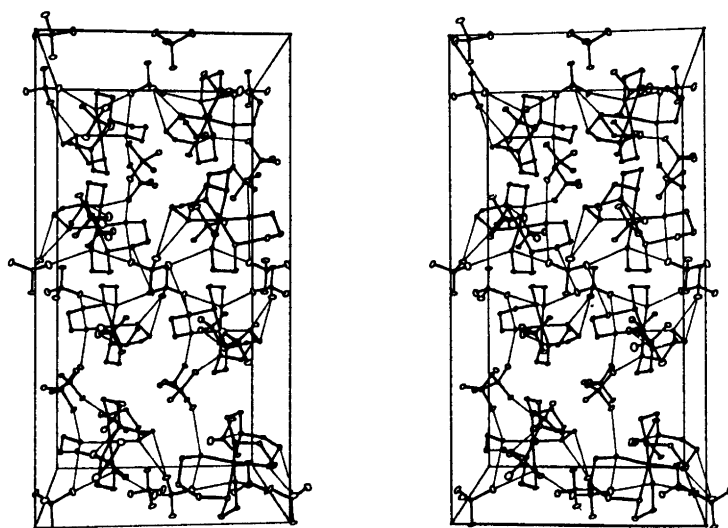


Fig. 10. Stereoscopic view along the *a*-axis of $[\text{Co}(\text{tacn})(\text{C-aeaps})](\text{ClO}_4)_2$. The disordered perchlorate ion is drawn with open bonds.

Also, the chemistry of Scheme 1 has been further investigated. An interesting crystal structure determination has been performed of a five-coordinate cobalt(III) compound which is the oxidized form of I with L = sulfite.²⁴ The authors maintain that the reaction of the cobalt(III) form of I to give II represents an electrophilic attack of Co(III) on the CH₂ group. However, in view of the results reported in this paper and in Ref. 12 it seems likely that Scheme 1 is a simple acid–base reaction. Owing to the low charge of I during the reaction one would expect much slower reaction with base than with our +3 charged coordination compound.

Acknowledgements. The authors thank Mr. Flemming Hansen for help during data collection and The Danish Natural Science Research Council for support. The Carlsberg Foundation is gratefully acknowledged for financial support and a grant for electrochemical equipment.

References

1. Kanamori, K., Broderick, W. E., Jordan, R. F., Willett, R. D. and Legg, J. I. *J. Am. Chem. Soc.* **108** (1986) 7122.
2. Bjerrum, M. J., Gajhede, M., Larsen, E. and Springborg, J. *Inorg. Chem.* **27** (1988) 3960.
3. Okamoto, M. S. and Barefield, E. K. *Inorg. Chim. Acta* **17** (1976) 91.
4. Searle, G. H. and Geue, R. J. *Austr. J. Chem.* **37** (1984) 959.
5. Searle, G. H. and Larsen, E. *Acta Chem. Scand., Ser. A30* (1976) 143.
6. Bjerrum, M. J., Laier, T. and Larsen, E. *Inorg. Chem.* **25** (1986) 816.
7. Bjerrum, M. J. and Larsen, E. *Acta Chem. Scand., Ser. A39* (1985) 465.
8. Doddrell, D. M., Pegg, D. T. and Bendall, M. R. *J. Magn. Reson.* **48** (1982) 323.
9. Belton, P. S., Cox, I. J. and Harris, R. K. *J. Chem. Soc., Faraday Trans. 2*, **81** (1985) 63.
10. *Structure Determination Package*. Enraf-Nonius, Delft, The Netherlands 1985.
11. Cromer, D. T. and Waber, J. T. *International Tables for X-Ray Crystallography*. The Kynoch Press, Birmingham 1974, Vol. IV.
12. Kofod, P., Larsen, E., Petersen, C. H. and Springborg, J. *Acta Chem. Scand.* *To be submitted*.
13. Harris, D. C. *Quantitative Chemical Analysis*, N. H. Freeman, San Francisco, CA 1982.
14. Willinski, J. and Kurland, R. J. *Inorg. Chem.* **12** (1973) 2202.
15. Comba, P. and Sargeson, A. M. *J. Chem. Soc., Chem. Commun.* (1975) 919.
16. Pyper, N. C. *Mol. Phys.* **19** (1970) 161.
17. Schrauzer, G. N. and Windgassen, R. J. *J. Am. Chem. Soc.* **88** (1966) 3738.
18. Hammershoi, A., Larsen, E. and Larsen, S. *Acta Chem. Scand., Ser. A32* (1978) 501.
19. Hammershoi, A. and Larsen, E. *Acta Chem. Scand., Ser. A32* (1978) 485.
20. Bjerrum, M. J., Laier, T. and Larsen, E. *Inorg. Chem.* **25** (1986) 816.
21. Taylor, R. and Kennard, O. *J. Am. Chem. Soc.* **104** (1982) 5063.
22. Blake, A. J., Holder, A. J., Hyde, T. I., Küppers, H.-J., Schröder, M., Stötzel, S. and Wieghardt, K. *J. Chem. Soc., Chem. Commun.* (1989) 1600.
23. Barbarella, G., Dembech, P., Garbesi, A., Bernardi, F., Bottoni, A. and Fava, A. *J. Am. Chem. Soc.* **100** (1978) 200.
24. Broderick, W. E., Kanamori, K., Willett, R. D. and Legg, J. I. *Inorg. Chem.* **30** (1991) 3875.

Received December 18, 1991.